

ARTICLE TYPE

Geometric Tracking Control of a Multi-rotor UAV for Partially Known Trajectories

Yogesh Kumar¹ | S.B. Roy¹ | P.B. Sujit²

¹ Department of Electronics and Communication Engineering, Indraprastha Institute of Information Technology Delhi, Delhi, India

² Department of Electrical Engineering and Computer Science, Indian Institute of Science Education and Research Bhopal, Madhya Pradesh, India

Correspondence

Corresponding author Yogesh Kumar,
Email: yogeshk@iiitd.ac.in

Abstract

This paper presents a trajectory-tracking controller for multi-rotor unmanned aerial vehicles (UAVs) in scenarios where only the desired position and heading are known without the higher-order derivatives. The proposed solution modifies the state-of-the-art geometric controller, effectively addressing challenges related to the non-existence of the desired attitude and ensuring positive total thrust input for all time. We tackle the additional challenge of the non-availability of the higher derivatives of the trajectory by introducing novel nonlinear filter structures. We formalize theoretically the effect of these filter structures on the system error dynamics. Subsequently, through a rigorous theoretical analysis, we demonstrate that the proposed controller leads to uniformly ultimately bounded system error dynamics.

KEY WORDS

Nonlinear control, geometric control, multi-rotor UAV, quadrotors, nonlinear filters on SO(3).

1 | INTRODUCTION

Multi-rotor unmanned aerial vehicles (UAVs) are becoming a commonplace operational necessity due to their dynamic capabilities, such as vertical take-off, landing, and hovering. Over the years, many developments in multi-rotor controller synthesis have occurred, especially for quadrotors considering various factors, including implementation complexity, required performance, and available computational resources¹. The commonly used multi-rotor UAVs are underactuated with highly non-linear and coupled dynamics, which demands special consideration when designing globally stable trajectory tracking controller².

While hardware and software advances are shrinking the gaps between theory and practice, the ever-increasing application domain introduces new challenges. One such challenge is to solve a tracking control problem where the desired trajectory is not fully known, especially for cases that require non-cooperative target tracking or coordination with other vehicles^{3,4}. Due to hardware or security considerations, obtaining complete information about the motion of the other vehicle other than the pose measurement is often challenging⁵. The non-cooperative tracking problem is usually tackled using the augmentation of vision sensors, such as - position-based visual servoing (PBVS)^{6,3,7} or image-based visual servoing (IBVS)^{8,9,10,11}.

Compensating for unknown target dynamics is a challenging issue that is often tackled by either introducing a robust conservative component in the controller or deriving feedback compensation for the target velocity based on ad-hoc techniques such as optical flow^{9,11,12} and Kalman filter^{3,13,8}, etc. while considering restrictive assumptions on the target motion. In our earlier work¹⁴, we proposed an IBVS method for quadrotors to overcome these challenges at the kinematic level. However, the internal attitude and translational controllers further require higher derivatives of the target dynamics. The knowledge of higher derivatives of target dynamics is thus necessary, and solutions such as high controller gain¹⁰ or command filter-based¹⁵ techniques¹⁶ are proposed in the literature. Recently, the authors in¹⁷ introduced a high gain controller based on the Euler angle formulation to address the requirement of higher derivatives of the target dynamics. However, Euler angle-based methods show singularities¹⁸, which restricts the UAV performance for nontrivial trajectories.

arXiv:2311.07331v1 [eess.SY] 13 Nov 2023

This paper proposes a solution to the general problem of designing a trajectory-tracking controller for the multi-rotor UAV when only the desired position and heading are available. We will design our controller by suitably modifying the state-of-the-art geometric controller proposed in^{18,19}. Developed on the special Euclidean group $SE(3)$, the geometric controller enables us to design an almost global trajectory tracking controller for multi-rotor UAVs. However, two major limitations of this controller are (i) the thrust is not saturated, hence no guarantee of the existence of the desired angular orientation, and (ii) the designed thrust can be negative when the angle between the third body axis of a multi-rotor UAV and desired thrust direction is greater than 90° ²⁰. Our proposed solution addresses these limitations in the current context of designing the controller for partially known trajectories.

The main contributions of the paper are as follows

- We consider the problem of multi-rotor tracking a partially known trajectory and develop a trajectory-tracking controller by suitably modifying the state-of-the-art geometric controller¹⁸.
- Unlike²¹, an auxiliary filter dynamics in $SO(3)$ space is proposed for the UAV attitude system, which tackle the requirement of higher-order derivatives of the desired position in desired attitude derivatives. A similar approach using command filter is presented in²²; however, considering a quaternion-based formulation. To the best of our knowledge, this is the first time the consequences of such filter dynamics for attitude representations in $SO(3)$ are quantified on the overall system through a Lyapunov-based analysis.
- To ensure the non-zero desired thrust requirements for the existence of the desired attitude^{10,23}, we propose a projection-based filter dynamics to yield a bounded second-order derivative of the desired position. Further, we discuss the effect of large attitude errors on the thrust control inputs proposed in^{18,20} in detail and introduce a novel control strategy.
- The effect of the proposed control scheme, along with the auxiliary filter dynamics, is theoretically analyzed. The overall system consisting of translational, angular, and auxiliary dynamics is shown to be uniformly ultimately bounded through rigorous mathematical arguments. The careful design and extensive theoretical analysis enable us with an ultimate bound that can be made arbitrarily small by choosing high enough auxiliary dynamics gains without burdening the controller gains.

The rest of the paper is organized as follows. Section 2 describes the problem formulation with the control objective. The controller design is presented in Section 3 followed by the theoretical analysis in Section 4. Finally, section 5 draws the conclusions.

2 | PROBLEM FORMULATION AND PRELIMINARIES

2.1 | Notations

The set of real numbers is represented as \mathbb{R} , while the set of positive real numbers as \mathbb{R}_+ . The identity matrix of size 3 is represented as I . Operators $\lambda_{max}(\cdot)$ and $\lambda_{min}(\cdot)$ represents the maximum and minimum eigenvalue of input matrix, respectively. The special orthogonal group $SO(3)$ which contains the orthogonal matrices is defined as

$$SO(3) = \{R \in \mathbb{R}^{3 \times 3} | R^T R = R R^T = I, \det(R) = 1\}. \quad (1)$$

The group of skew-symmetric matrices $\mathfrak{so}(3)$ is defined as

$$\mathfrak{so}(3) = \{S \in \mathbb{R}^{3 \times 3} | S = -S^T\}. \quad (2)$$

Map $(\cdot) : \mathbb{R}^3 \rightarrow \mathfrak{so}(3)$ is the skew-symmetric map whereas it's inverse is denoted by $(\cdot)^\vee : \mathfrak{so}(3) \rightarrow \mathbb{R}^3$ and $e_3 = [0, 0, 1]^T$. For a vector v , $\|v\|$ denotes the 2-norm whereas for a matrix M , $\|M\|$ denotes the 2-norm until unless specified. $\ln(\cdot)$ represents the natural logarithmic operator. For a vector $v = [v_1, v_2, v_3]^T$,

$$\tanh(v) = [\tanh(v_1), \tanh(v_2), \tanh(v_3)]^T \in \mathbb{R}^3, \quad (3)$$

$$\text{Cosh}(v) = \text{diag}\{\cosh(v_1), \cosh(v_2), \cosh(v_3)\} \in \mathbb{R}^{3 \times 3}, \quad (4)$$

$$\text{Tanh}(v) = \text{diag}\{\tanh(v_1), \tanh(v_2), \tanh(v_3)\} \in \mathbb{R}^{3 \times 3}. \quad (5)$$

$$\text{Sech}(v) = \text{Cosh}^{-1}(v). \quad (6)$$

2.2 | Multi-rotor Dynamics

Consider a multi-rotor UAV illustrated in Figure 1. Let $\{I\}$ and $\{B\}$ be the inertial and the vehicle body frames, with origins O_I and O_B , respectively. The configuration of UAV is defined by the position $x \in \mathbb{R}^3$ of the center of mass and attitude $R = [x_B, y_B, z_B] \in SO(3)$ in the inertial frame.

We model the multi-rotor dynamics as

$$\dot{x} = v, \quad (7)$$

$$m\dot{v} = mge_3 - fRe_3, \quad (8)$$

$$\dot{R} = R\hat{\Omega}, \quad (9)$$

$$J\dot{\Omega} = -\Omega \times J\Omega + M, \quad (10)$$

where inertial frame position $x(t) \in \mathbb{R}^3$, inertial frame velocity $v(t) \in \mathbb{R}^3$, the rotation matrix from $\{B\}$ to $\{I\}$, $R(t) \in SO(3)$ and the body-fixed angular velocity $\Omega(t) \in \mathbb{R}^3$ represents the multi-rotor states. The total thrust $f \in \mathbb{R}$ and moment $M = [M_1, M_2, M_3]^T \in \mathbb{R}^3$ expressed in body frame, are considered as the control inputs to the multi-rotor model. For a given pair of total thrust and moment, the rotor speeds can be calculated using the following relation

$$\begin{bmatrix} f \\ M \end{bmatrix} = \Gamma \omega_T, \quad \omega_T = [\omega_1^2, \dots, \omega_n^2]^T, \quad (11)$$

where n is the number of rotors and $\Gamma \in \mathbb{R}^{4 \times n}$ is a constant mixing matrix constructed based on the rotor configuration parameters such as placement of rotors, thrust, and moment coefficient of rotors etc².

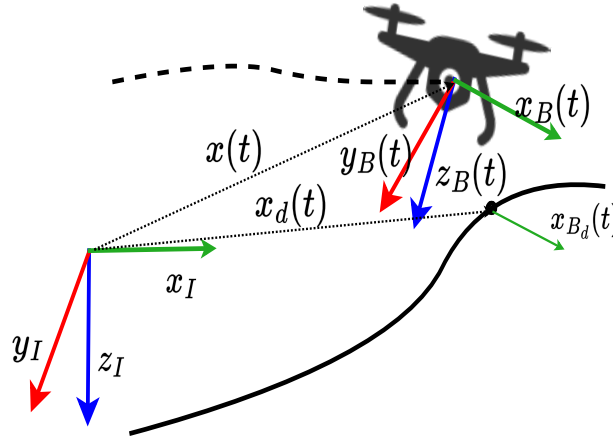


FIGURE 1 Coordinate frames illustration. The x , y , z axes of a coordinate frame $\{A\}$ are denoted by x_A , y_A and z_A , respectively.

2.3 | Control Objective

The objective is to design a nonlinear trajectory tracking controller for a multi-rotor UAV to track a position reference $x_d(t)$ and a heading direction $x_{B_d}(t)$ or a heading angle $\psi_d(t)$, where $x_{B_d}(t) = [\cos\psi_d(t), \sin\psi_d(t), 0]^T$. Moreover, we consider that the higher derivatives of the position reference and heading direction (i.e. $\frac{d^n x_d(t)}{dt^n}$ and $\frac{d^n x_{B_d}(t)}{dt^n}$, $n \geq 1$) are not available, which are essential for an accurate and efficient trajectory tracking controller.

Assumption 1. We assume that the reference trajectory has bounded derivatives as

$$\sup_{t \geq 0} \left\| \frac{d^n x_d(t)}{dt^n} \right\| = h_n, \quad n = 1, 2, 3, 4, \quad \sup_{t \geq 0} \left\| \frac{dx_{B_d}(t)}{dt} \right\| = h_5, \quad \sup_{t \geq 0} \left\| \frac{d^2 x_{B_d}(t)}{dt^2} \right\| = h_6. \quad (12)$$

where $h_1, h_2, h_3, h_4, h_5, h_6 \in \mathbb{R}_+$ are finite constants.

3 | CONTROL DESIGN

We follow a multistage procedure illustrated in Figure 2 to design the trajectory tracking controller. We first design the position tracking controller to obtain the control input $f(t)$. Subsequently, a desired rotation matrix $R_c(t) \in \text{SO}(3)$ constructed exploiting unit vector direction of f and desired heading direction $x_{B_d}(t)$. We then pass $R_c(t)$ through an auxiliary filter dynamics to obtain the filtered desired attitude reference, which the proposed attitude tracking controller would track.

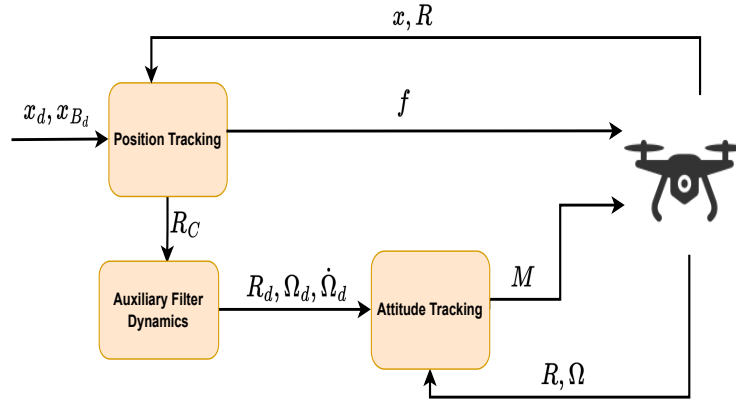


FIGURE 2 Control architecture

3.1 | Position Tracking Controller

To design a smooth, saturated position tracking controller, we consider an error system²³ with position tracking error $e_x(t)$ and filter tracking error $e_\alpha(t)$ as

$$e_x = x - x_d = [e_{x_1}, e_{x_2}, e_{x_3}]^T, \quad (13)$$

$$e_\alpha = \dot{e}_x + \alpha_x \tanh(e_x) + \tanh(e_f), \quad (14)$$

where $e_f(t) = [e_{f_x}(t), e_{f_y}(t), e_{f_z}(t)]^T$ is an auxiliary filter variable with the dynamics

$$\dot{e}_f = \text{Cosh}^2(e_f) (-k_\alpha e_\alpha + \tanh(e_x) - \alpha_f \tanh(e_f)), \quad (15)$$

and $\{k_\alpha, \alpha_f, \alpha_x \in \mathbb{R}_+\}$ are positive constant control design parameters.

The thrust control input $f(t)$ is designed as

$$f = \|f_d\| \sqrt{\frac{1 + e_3^T R_c^T R e_3}{2}} \quad (16)$$

where $f_d(t)$ is a virtual control input defined as

$$f_d = mge_3 - mg_1 + 2m \tanh(e_x) - mk_\alpha \tanh(e_f), \quad (17)$$

and $g_1(t)$ is an estimate of $\ddot{x}_d(t)$ which is not directly available and R_c is the desired attitude matrix carefully constructed in the subsequent section. Note that the thrust expression requires term \dot{e}_x , i.e., velocity feedback, in the e_f . Since we don't have the explicit knowledge of \dot{x}_d , one can circumvent the requirement of unknown term \dot{e}_x in thrust input calculation following the output-feedback formulation in²⁴. This also makes the position dynamics loop output feedback.

3.2 | Estimate of $\ddot{x}_d(t)$

To obtain the smooth and bounded estimate $g_1(t)$ of $\ddot{x}_d(t)$, we start by considering the following filter structure with filter input $x_d(t)$ and output $x_{f_d}(t)$

$$\gamma_1 \dot{x}_{f_d} + x_{f_d} = x_d, \quad x_{f_d}(0) = 0. \quad (18)$$

Consider another filter with filter design parameter $\gamma_1 \in \mathbb{R}_+$ to filter the unknown variable $\dot{x}_d(t)$ as

$$\gamma_1 \dot{g}_{x_d} + g_{x_d} = \dot{x}_d, \quad g_{x_d}(0) = 0. \quad (19)$$

Integrating (19) for $g_{x_d}(t)$ yield

$$g_{x_d}(t) = \frac{1}{\gamma_1} \left(x_d(t) - x_{f_d}(t) - \exp\left(-\frac{1}{\gamma_1}t\right)x_d(0) \right). \quad (20)$$

Since $g_{x_d}(t)$ represents the filtered output of unknown variable $\dot{x}_d(t)$, we further pass it through a filter with design parameter $\gamma_2 \in \mathbb{R}_+$ as

$$\gamma_2 \dot{g}_{f_d} + g_{f_d} = g_{x_d}, \quad g_{f_d}(0) = 0, \quad (21)$$

to obtain the estimate of $\ddot{x}_d(t)$. Further following the filter structure similar to (19) for the unknown variable \dot{g}_{x_d} and integrating it for its filter variable $g_{v_d}(t)$, we get

$$g_{v_d}(t) = \frac{1}{\gamma_2} \left(g_{x_d}(t) - g_{f_d}(t) - \exp\left(-\frac{1}{\gamma_2}t\right)g_{x_d}(0) \right). \quad (22)$$

For clarity, the filter structures discussed above are illustrated in Figure 3. Filter block 1 includes structures given by equations (18) and (20), with input $x_d(t)$ and output signal $g_{x_d}(t)$. Similarly, filter block 2 takes $g_{x_d}(t)$ as input and provides $g_{v_d}(t)$ using equations (21) and (22).

Following the rigorous analysis presented in the subsequent sections, we can use $g_{v_d}(t)$ as an estimate of $\ddot{x}_d(t)$, however, this estimate can suffer from peaking phenomenon due to the low value of γ_2 which might jeopardize the saturated thrust requirements to design a smooth attitude tracking controller. To get a saturated thrust input, a differential projection filter for a bounded estimate $g_1(t)$ of $\ddot{x}_d(t)$ with design parameter $\gamma_{21} \in \mathbb{R}_+$ and $g_1(0) = 0$ is proposed as

$$\dot{g}_1 = Proj(g_1, \phi) = \begin{cases} \phi - \frac{\nabla f(g_1)(\nabla f(g_1))^T}{\|\nabla f(g_1)\|^2} \phi f(g_1), & \text{if } f(g_1) > 0 \text{ \& } \phi^T \nabla f(g_1) > 0 \\ \phi, & \text{otherwise} \end{cases}, \quad (23)$$

where

$$\phi = \frac{1}{\gamma_{21}}(g_{v_d} - g_1), f(g_1) = \frac{\|g_1\|^2 - h_2^2}{\epsilon_0 h_2^2}, \nabla f(g_1) = \frac{2g_1}{\epsilon_0 h_2^2},$$

where h_2 is the known upper bound of the \ddot{x}_d and $\epsilon_0 > 0$ is the tolerance.

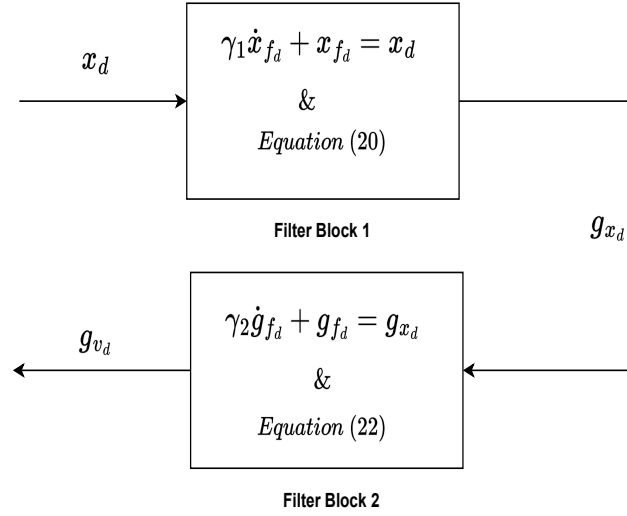


FIGURE 3 Filters illustration

3.3 | Auxiliary Desired Attitude Construction

The desired attitude $R_c(t)$ is constructed exploiting the virtual control input $f_d(t)$ given in (17) and the desired heading direction $x_{B_d}(t)$ as

$$R_c = [x_{B_c}, y_{B_c}, z_{B_c}], \quad (24)$$

$$z_{B_c} = \frac{f_d}{\|f_d\|} \quad y_{B_c} = -\frac{x_{B_d} \times z_{B_c}}{\|x_{B_d} \times z_{B_c}\|} \quad x_{B_c} = y_{B_c} \times z_{B_c}. \quad (25)$$

Once we construct the desired attitude matrix a well defined[‡] $R_c(t)$ as given in (24), the desired angular velocity $\Omega_c(t)$ and acceleration $\hat{\Omega}_c(t)$ corresponding to this can be calculated as

$$\hat{\Omega}_c = R_c^T \dot{R}_c, \quad (26)$$

$$\dot{\hat{\Omega}}_c = R_c^T \ddot{R}_c - \hat{\Omega}_c^2, \quad (27)$$

Note that the above calculations are essential to design an accurate attitude tracking control law for the dynamics given in (9) and (10)^{18,19}. However, one requires information about the higher derivatives of the virtual input $f_d(t)$ and heading direction $x_{B_d}(t)$ to calculate \dot{R}_c, \ddot{R}_c . Providing the information mentioned earlier is not feasible as it involves higher derivatives of the desired trajectory and even the multi-rotor UAV's states such as rate of acceleration (jerk). This issue is tackled by systematically defining an appropriate auxiliary filter dynamics for the available signal $R_c(t) \in SO(3)$ to obtain a filtered signal $R_d(t) \in SO(3)$ strictly belonging to the special orthogonal group and an angular velocity $\Omega_d(t)$ associated to it as

$$\dot{R}_d = R_d \hat{\Omega}_d, \quad (28)$$

$$\dot{\hat{\Omega}}_d = -\frac{1}{\gamma_4} e_{\Omega_{dc}} + e_R(R_d, R_c) + \frac{1}{\gamma_3} E(R_d, R_c) \Omega_d, \quad (29)$$

where $e_R(R_d, R_c)$ is the attitude error between R_c and R_d as described in Appendix A. $\gamma_3, \gamma_4 \in \mathbb{R}_+$ are the constant design parameters. The term $E(R_d, R_c)$ is also described in Appendix A. The error $e_{\Omega_{dc}} = \Omega_d + \frac{1}{\gamma_3} e_{R_{dc}}$ is carefully designed based on the stability analysis in the subsequent section.

[‡] We assume that $x_{B_d}(t) \nparallel z_{B_c}(t)$. We note that one can circumvent this singularity in differential flatness transformation using the Hopf Fibration on $SO(3)$ proposed in [25]. However this is out of scope of the current problem formulation.

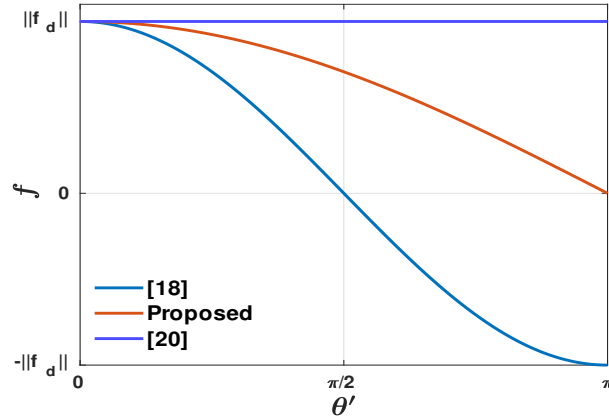


FIGURE 4 Thrust control input comparison. θ' is the angle between z_{B_c} and z_B .

3.4 | Effect of large attitude errors on f

Authors in¹⁸ discussed the necessity of designing the thrust control input f to reduce its magnitude whenever there are large attitude errors. They do so by multiplying the magnitude of the virtual control input f_d with the dot product of $z_{B_c} = R_c e_3$ and $z_B = R e_3$, i.e., $f = \|f_d\| e_3^T R_c^T R e_3$. The term $e_3^T R_c^T R e_3$ represents the cosine of the angle between z_{B_c} and z_B , which can make the control input f negative whenever the angle is greater than 90° , which is not feasible for the quadrotor to attain. To address this, authors in²⁰ suggested using simply the magnitude of the virtual control input, i.e., $f = \|f_d\|$ as the thrust control input. However, this may cause instability in the overall system dynamics by generating unnecessarily high thrust for large attitude errors. The careful analysis and design of the thrust control input in equation (16) attenuates both of these problems by multiplying the scaling quantity $\sqrt{\frac{1+e_3^T R_c^T R e_3}{2}}$ to $\|f_d\|$ which is nothing but cosine of half of the angle between z_{B_c} and z_B . An illustrative comparison of different thrust inputs with the respective virtual control inputs in the case of^{18, 20} and the proposed method w.r.t to the angle between z_{B_c} and z_B is provided in Figure 4.

Remark 1. Note that the proposed virtual control input (17) is always positive for a tunable k_α , which is a necessary condition for the existence of the desired attitude $R_c(t)$. Moreover, the requirement of proportionally reduced thrust magnitude for large attitude error is inherently captured in the designed thrust input (16) in the whole configuration space (especially angles greater than 90°).

3.5 | Attitude Tracking Controller

We now design the attitude control input M ¹⁹ to track the auxiliary reference signals $R_d(t), \Omega_d(t), \dot{\Omega}_d(t)$ as follows

$$M = -k_R e_R(R, R_d) - k_\Omega e_\Omega(R, \Omega, R_d, \Omega_d) + \Omega \times J\Omega - J(\hat{\Omega} R^T R_d \Omega_d - R^T R_d \dot{\Omega}_d), \quad (30)$$

where $\{k_R, k_\Omega \in \mathbb{R}_+\}$ are constant control design parameters. The attitude and angular velocity errors $e_R(R, R_d)$ and $e_\Omega(R, \Omega, R_d, \Omega_d)$ are defined in detail in Appendix A.

4 | THEORETICAL ANALYSIS

To comment on the stability and error convergence of the complete system, we first derive the comprehensive closed-loop error dynamics for individual subsystems.

4.1 | Position Tracking Error System

Using the relations given in (13) and (14) the time derivative of e_x can be given as

$$\dot{e}_x = e_\alpha - \alpha_x \tanh(e_x) - \tanh(e_f). \quad (31)$$

The open-loop dynamics of the filter tracking error multiplied by mass $me_\alpha(t)$ substituting the system dynamics (8) and auxiliary filter dynamics (15) can be written as

$$m\dot{e}_\alpha = mge_3 - fRe_3 - m\ddot{x}_d + \chi - mk_\alpha e_\alpha + m \tanh(e_x) \quad (32)$$

where $\chi = m\alpha_x \text{Sech}^2(e_x)\dot{e}_x - m\alpha_f \tanh(e_f)$. To better understand the attitude dynamics coupling, the virtual control input $f_d(t)$ is added and subtracted to the right-hand side of (32) as

$$m\dot{e}_\alpha = mge_3 + \Delta f + \chi - m\ddot{x}_d - mk_\alpha e_\alpha + m \tanh(e_x) - f_d, \quad (33)$$

where $\Delta f = f_d - fRe_3$.

Using the expression for virtual control input from (17), the closed-loop filter error dynamics can be written as

$$m\dot{e}_\alpha = \Delta f + \chi - m(\ddot{x}_d - g_1) - mk_\alpha e_\alpha - m \tanh(e_x) + mk_\alpha \tanh(e_f). \quad (34)$$

To analyze the dynamical behavior of the proposed filter structures for desired position reference derivatives $\frac{d^n x_d(t)}{dt^n}$, we propose the following error system $e_d(t)$ as

$$e_d = \begin{bmatrix} e_{g_x} \\ e_{\ddot{x}_d} \\ e_{g_v} \\ e_{g_1} \end{bmatrix} = \begin{bmatrix} \dot{x}_d - g_{x_d} \\ \ddot{x}_d - \dot{g}_{x_d} \\ \dot{g}_{x_d} - g_{v_d} \\ \ddot{x}_d - g_1 \end{bmatrix}. \quad (35)$$

Using the expressions from (18), (19), (21) and (23), the closed loop error dynamics for error system (35) can be given as

$$\begin{bmatrix} \dot{e}_{g_x} \\ \dot{e}_{\ddot{x}_d} \\ \dot{e}_{g_v} \\ \dot{e}_{g_1} \end{bmatrix} = \begin{bmatrix} -\frac{1}{\gamma_1} e_{g_x} + \ddot{x}_d \\ -\frac{1}{\gamma_1} e_{\ddot{x}_d} + \ddot{\ddot{x}}_d \\ -\frac{1}{\gamma_2} e_{g_v} + \frac{1}{\gamma_1} e_{\ddot{x}_d} \\ -\frac{1}{\gamma_{21}} e_{g_1} + \frac{1}{\gamma_{21}} e_{g_v} + \frac{1}{\gamma_{21}} e_{\ddot{x}_d} + \Phi_{g_1} + \ddot{\ddot{x}}_d \end{bmatrix} \quad (36)$$

where

$$\Phi_{g_1} = \frac{\nabla f(g_1)(\nabla f(g_1))^T}{\|\nabla f(g_1)\|^2} \phi f(g_1) \quad (37)$$

which appears only if $f(g_1) > 0$ & $\phi^T \nabla f(g_1) > 0$. Moreover, $e_{g_1}^T \Phi_{g_1} \leq 0$ (Please refer to the properties of projection in²⁵).

4.2 | Attitude Tracking Error System

The time derivatives of the attitude error system with its properties are discussed in detail in Appendix A, which will be helpful in the theoretical claims provided in this section. For simplicity in the representation, we will use the following notations for the various attitude and angular velocity errors throughout the paper.

$$e_R(R, R_d) = e_{R_d}, \quad e_R(R, R_c) = e_{R_c}, \quad e_R(R_d, R_c) = e_{R_{dc}}, \quad e_\Omega(R, \Omega, R_d, \Omega_d) = e_{\Omega_d}. \quad (38)$$

Using the control input M , the closed loop error dynamics of angular error e_{Ω_d} premultiplied with inertia matrix J can be given as

$$J\dot{e}_{\Omega_d} = -k_R e_{R_d} - k_\Omega e_{\Omega_d}. \quad (39)$$

4.3 | Stability Analysis

The stability and convergence analysis is systematically presented in this section. We first state the following lemmas, which will be utilized in the subsequent analysis.

Lemma 1. *There exist positive constants α_1, α_2 such that*

$$\|f_d\| \leq \alpha_1, \quad \|f_d\| \geq \alpha_2. \quad (40)$$

Further, α_2 is strictly positive if

$$k_\alpha < g - h_2 - 2. \quad (41)$$

Proof. Please refer to Appendix B.1 for the proof. \square

Lemma 2. *The quantity $\Delta f = f_d - fRe_3$ satisfies the following bound*

$$\|\Delta f\| \leq 2\alpha_1(\|e_{R_d}\| + \|e_{R_d}\|). \quad (42)$$

Proof. Please refer to Appendix B.2 for the proof. \square

Lemma 3. *The desired angular velocity Ω_c satisfies the following bound*

$$\|\hat{\Omega}_c\| \leq \rho_1(\|e_\alpha\|, \|\tanh(e_x)\|, \|\tanh(e_f)\|) + \rho_{01}. \quad (43)$$

Proof. Please refer to Appendix B.3 for the proof. \square

Lemma 4. *The filter errors given in equation (36) can be bounded as*

$$\|e_{g_x}(t)\| \leq \sqrt{\|e_{g_x}(0)\|^2 \exp\left(-\frac{1}{\gamma_1}t\right) + \gamma_1^2 h_2^2} \leq \max(\|e_{g_x}(0)\|, \gamma_1 h_2) = \alpha_3, \quad (44)$$

$$\|e_{\ddot{x}_d}(t)\| \leq \sqrt{\|e_{\ddot{x}_d}(0)\|^2 \exp\left(-\frac{1}{\gamma_1}t\right) + \gamma_1^2 h_3^2} \leq \max(\|e_{\ddot{x}_d}(0)\|, \gamma_1 h_3) = \alpha_4, \quad (45)$$

$$\|e_{g_v}(t)\| \leq \sqrt{\|e_{g_v}(0)\|^2 \exp\left(-\frac{1}{\gamma_2}t\right) + \frac{\gamma_2^2}{\gamma_1^2} \|e_{\ddot{x}_d}\|^2} \leq \max\left(\|e_{g_v}(0)\|, \frac{\gamma_2}{\gamma_1} \max(e_{\ddot{x}_d}(0), \gamma_1 h_3)\right) = \alpha_5, \quad (46)$$

$$\|e_{g_1}(t)\| \leq \max\left(\|e_{g_1}(0)\|, \sqrt{8(\alpha_4^2 + \alpha_5^2) + 2\gamma_{21}^2 h_3^2}\right) = \alpha_6. \quad (47)$$

Proof. Please refer to Appendix B.4 for the proof. \square

Next, we derive the stability and convergence properties of the attitude subsystem of the multirotor tracking the auxiliary desired attitude.

Theorem 1. (Adapted from¹⁹) *The closed loop error dynamics of $e_1(t) = [e_{R_d}(t)^T, e_{\Omega_d}(t)^T]^T$ is exponentially stable with the control input M defined in (30) for the smooth desired attitude reference $(R_d(t), \Omega_d(t), \dot{\Omega}_d(t))$. Moreover, an estimate of the region of attraction is given by*

$$\Psi(R(0), R_d(0)) < 2, \quad (48)$$

$$\|e_{\Omega_d}(0)\|^2 < \frac{2k_R}{\lambda_{\max}(J)} (2 - \Psi(R(0), R_d(0))). \quad (49)$$

Proof. We start by proving that given condition (49), the sublevel set $\mathcal{L}_2 = \{R, R_d \in \text{SO}(3) | \Psi(R, R_d) < 2\}$ is positively invariant set. Consider the following Lypunov candidate

$$V_1 = \frac{1}{2} e_{\Omega_d}^T e_{\Omega_d} + k_R \Psi(R, R_d) \quad (50)$$

Taking the time derivative of $V_1(t)$ after substituting the dynamics (39) and (A4) yields

$$\dot{V}_1 = -k_\Omega \|e_{\Omega_d}\|^2. \quad (51)$$

Equation (51) along with (48) and (49) implies that

$$k_R \Psi(R(t), R_d(t)) \leq V_1(t) \leq V_1(0) < 2k_R \quad \forall t > 0. \quad (52)$$

This proves that the sub-level set \mathcal{L}_2 is a positively invariant set such that $\Psi(R(t), R_d(t)) < 2$ and hence the attitude errors are well defined.

To prove the exponential stability, let's consider another Lyapunov candidate

$$V_2 = \frac{1}{2} e_{\Omega_d}^T e_{\Omega_d} + k_R \Psi(R, R_d) + c_1 e_{R_d}^T e_{R_d}, \quad (53)$$

where c_1 is a positive constant. Using the properties of configuration error function, for $e_1(t) = [e_{R_d}(t)^T, e_{\Omega_d}(t)^T]^T$ we get

$$e_1^T W_{11} e_1 \leq V_1 \leq e_1^T W_{12} e_1, \quad (54)$$

where

$$W_{11} = \begin{bmatrix} k_R & \frac{c_2}{2} \\ \frac{c_2}{2} & \lambda_{\min}(J) \end{bmatrix}, \quad W_{12} = \begin{bmatrix} 2k_R & \frac{c_2}{2} \\ \frac{c_2}{2} & \lambda_{\max}(J) \end{bmatrix}. \quad (55)$$

Taking time derivative of $V_2(t)$ and substituting the appropriate error dynamics using (39), (A4) and (A5) will yield

$$\dot{V}_2 = -k_\Omega e_{\Omega_d}^T e_{\Omega_d} - c_1 k_R e_{R_d}^T J^{-1} e_{R_d} + c_1 k_\Omega e_{R_d}^T J^{-1} e_{\Omega_d} + c_1 e_{\Omega_d}^T E^T(R, R_d) e_{\Omega_d}. \quad (56)$$

Further taking bounds using the properties in Appendix A in equation (56) will yield

$$\dot{V}_2 \leq - \underbrace{\left[k_\Omega - \frac{c_1}{2} - \frac{c_1 k_\Omega}{2\lambda_{\min}(J)} \right]}_{\bar{\lambda}_1} \|e_{\Omega_d}\|^2 - \underbrace{\left[\frac{c_1 k_R}{\lambda_{\max}(J)} - \frac{c_1 k_\Omega}{2\lambda_{\min}(J)} \right]}_{\bar{\lambda}_2} \|e_{R_d}\|^2. \quad (57)$$

Furthermore, we can write

$$\dot{V}_2 \leq -\bar{\beta} V_2, \quad (58)$$

where $\bar{\beta} = \frac{\min(\bar{\lambda}_1, \bar{\lambda}_2)}{\lambda_{\max}(W_{12})}$. We choose the parameter so that $\bar{\beta}$ is positive. Then, the relation (58) invokes global uniform exponential stability (based on Theorem 4.10 in²⁶). \square

Now, we are ready to state our main results.

Theorem 2. Consider the multi-rotor dynamics (7), (8), (9) and (10), with control inputs (16) and (30). The closed loop dynamics of overall system errors $e(t) = [e_1(t)^T, e_2(t)^T, e_3(t)^T]^T$ where $e_1(t) = [e_{R_d}(t)^T, e_{\Omega_d}(t)^T]^T$, $e_2(t) = [e_{R_{dc}}^T(t), e_{\Omega_{dc}}^T(t)]^T$ and

$e_3(t) = [e_\alpha^T(t), \tanh(e_x(t))^T, \tanh(e_f(t))^T]^T$, is uniformly ultimately bounded, provided the following gain conditions are satisfied

$$mk_\alpha - \frac{m\alpha_x(3\alpha_x + 1)}{2} - \frac{m\alpha_f}{2} - \rho_{03} > 0, \quad (59)$$

$$m\alpha_x - \frac{m\alpha_x^2}{2} > 0, \quad (60)$$

$$\frac{1}{2\gamma_3} - 2\alpha_1^2 > 0, \quad (61)$$

$$\frac{m\alpha_f}{2} - \frac{m\alpha_x}{2} > 0, \quad (62)$$

$$k_\Omega - \frac{c_1}{2} - \frac{c_1 k_\Omega}{2\lambda_{\min}(J)} > 0, \quad (63)$$

$$\frac{c_1 k_R}{\lambda_{\max}(J)} - \frac{c_1 k_\Omega}{2\lambda_{\min}(J)} - 2\alpha_1^2 > 0, \quad (64)$$

where the constant ρ_{03} is defined subsequently.

Proof. For the sake of simplicity, we proceed in the following steps to prove the theorem claims.

4.3.1 | Step 1

Let's first consider the Lyapunov candidate $V_3(t)$ for the translational error $e_3(t)$ of multi-rotor

$$V_3 = \frac{1}{2} m e_\alpha^T e_\alpha + m \ln(\cosh(e_{x_1})) + m \ln(\cosh(e_{x_2})) + m \ln(\cosh(e_{x_3})) + \frac{1}{2} m \tanh(e_f)^T \tanh(e_f). \quad (65)$$

Taking the time derivative of $V_3(t)$ and substituting equations (15), (31) and (34) yields

$$\begin{aligned} \dot{V}_3 = & -mk_\alpha e_\alpha^T e_\alpha + e_\alpha^T \Delta f + e_\alpha^T \chi - m e_\alpha^T e_{g_1} - m e_\alpha^T \tanh(e_x) + mk_\alpha e_\alpha^T \tanh(e_f) \\ & + m \tanh^T(e_x) (e_\alpha - \alpha_x \tanh(e_x) - \tanh(e_f)) + m \tanh(e_f)^T (-k_\alpha e_\alpha + \tanh(e_x) - \alpha_f \tanh(e_f)) \end{aligned} \quad (66)$$

Further solving (66) and taking bounds on $\dot{V}_3(t)$ yield

$$\dot{V}_3 \leq -mk_\alpha \|e_\alpha\|^2 - m\alpha_x \|\tanh(e_x)\|^2 - m\alpha_f \|\tanh(e_f)\|^2 + \|e_\alpha\| \|\Delta f\| + \|e_\alpha\| \|\chi\| + m \|e_\alpha\| \|e_{g_1}\|. \quad (67)$$

Solving equation (67) by substituting the dynamics of $\dot{e}_x(t)$ from (31) in χ , and using equations (42) and (47) produces

$$\begin{aligned} \dot{V}_3 \leq & -mk_\alpha \|e_\alpha\|^2 - m\alpha_f \|\tanh(e_f)\|^2 + \|e_\alpha\| (m\alpha_x \|\text{Sech}^2(e_x)\| \|\tanh(e_f)\| + m\alpha_f \|\tanh(e_f)\|) - m\alpha_x \|\tanh(e_x)\|^2 \\ & + \|e_\alpha\| \|\text{Sech}^2(e_x)\| (m\alpha_x \|e_\alpha\| + m\alpha_x^2 \|\tanh(e_x)\|) + m \|e_\alpha\| (\alpha_6 + 2\alpha_1 \|e_\alpha\| (\|e_{R_{dc}}\| + \|e_{R_d}\|)), \end{aligned} \quad (68)$$

which modifies to,

$$\begin{aligned} \dot{V}_3 \leq & -mk_\alpha \|e_\alpha\|^2 - m\alpha_x \|\tanh(e_x)\|^2 - m\alpha_f \|\tanh(e_f)\|^2 + m\alpha_x \|e_\alpha\|^2 + m\alpha_x^2 \|e_\alpha\| \|\tanh(e_x)\| \\ & + m\alpha_x \|e_\alpha\| \|\tanh(e_f)\| + m\alpha_f \|e_\alpha\| \|\tanh(e_f)\| + m \|e_\alpha\| \alpha_6 + 2\alpha_1 \|e_\alpha\| (\|e_{R_{dc}}\| + \|e_{R_d}\|), \\ \leq & -mk_\alpha \|e_\alpha\|^2 - m\alpha_x \|\tanh(e_x)\|^2 - m\alpha_f \|\tanh(e_f)\|^2 + m\alpha_x \|e_\alpha\|^2 + \frac{m\alpha_x^2}{2} \|e_\alpha\|^2 + \frac{m\alpha_x^2}{2} \|\tanh(e_x)\|^2 + \frac{m\alpha_x}{2} \|e_\alpha\|^2 \\ & + \frac{m\alpha_x}{2} \|\tanh(e_f)\|^2 + \frac{m\alpha_f}{2} \|e_\alpha\|^2 + \frac{m\alpha_f}{2} \|\tanh(e_f)\|^2 + \frac{m}{2} \|e_\alpha\|^2 + \frac{m}{2} \alpha_6^2 + \|e_\alpha\|^2 + 2\alpha_1^2 \|e_{R_{dc}}\|^2 + 2\alpha_1^2 \|e_{R_d}\|^2. \end{aligned} \quad (69)$$

Further manipulation yield

$$\begin{aligned} \dot{V}_3 \leq & - \left(mk_\alpha - m\alpha_x - \frac{m\alpha_x^2}{2} - \frac{m\alpha_x}{2} - \frac{m\alpha_f}{2} - \frac{m}{2} - 1 \right) \|e_\alpha\|^2 - \left(m\alpha_x - \frac{m\alpha_x^2}{2} \right) \|\tanh(e_x)\|^2 \\ & - \left(m\alpha_f - \frac{m\alpha_x}{2} - \frac{m\alpha_f}{2} \right) \|\tanh(e_f)\|^2 + 2\alpha_1^2 \|e_{R_{dc}}\|^2 + 2\alpha_1^2 \|e_{R_d}\|^2 + \frac{m}{2} \alpha_6^2. \end{aligned} \quad (70)$$

4.3.2 | Step 2

Now, let's consider another Lyapunov candidate $V_4(t)$ for auxiliary attitude errors $e_2(t)$ as

$$V_4(t) = \Psi(R_d, R_c) + \frac{1}{2} e_{\Omega_{dc}}^T e_{\Omega_{dc}}, \quad (71)$$

Taking the time derivative and using equations (28), (29), (A4), (A5) and (A6) yields

$$\dot{V}_4(t) = -\frac{1}{\gamma_3} e_{R_{dc}}^T e_{R_{dc}} - \frac{1}{\gamma_4} e_{\Omega_{dc}}^T e_{\Omega_{dc}} - e_{R_{dc}}^T R_d^T R_c \Omega_c + \frac{1}{\gamma_3} e_{\Omega_{dc}}^T E(R_d, R_c) R_d^T R_c \Omega_c \quad (72)$$

Taking bounds on $\dot{V}_4(t)$ yields

$$\dot{V}_4(t) \leq -\frac{1}{2\gamma_3} \|e_{R_{dc}}\|^2 - \frac{1}{2\gamma_4} \|e_{\Omega_{dc}}\|^2 + \left(\frac{\gamma_3}{2} + \frac{\gamma_4}{8\gamma_3^2}\right) \|\Omega_c\|^2 \quad (73)$$

4.3.3 | Step 3

To prove the stability of dynamics of error $e(t)$, let's consider the Lyapunov candidate as

$$V = V_2(t) + V_3(t) + V_4(t) \quad (74)$$

Taking the derivative of $V(t)$ using (73), (70) and (57) yields

$$\begin{aligned} \dot{V} \leq & -\left(mk_\alpha - m\alpha_x - \frac{m\alpha_x^2}{2} - \frac{m\alpha_x}{2} - \frac{m\alpha_f}{2} - \frac{m}{2} - 1\right) \|e_\alpha\|^2 - \left(m\alpha_x - \frac{m\alpha_x^2}{2}\right) \|\tanh(e_x)\|^2 \\ & - \left(m\alpha_f - \frac{m\alpha_x}{2} - \frac{m\alpha_f}{2}\right) \|\tanh(e_f)\|^2 + \frac{m}{2} \alpha_6^2 - \left(\frac{1}{2\gamma_3} - 2\alpha_1^2\right) \|e_{R_{dc}}\|^2 + \left(\frac{\gamma_3}{2} + \frac{\gamma_4}{8\gamma_3^2}\right) \|\Omega_c\|^2 \\ & - \left(k_\Omega - \frac{c_1}{2} - \frac{c_1 k_\Omega}{2\lambda_{\min}(J)}\right) \|e_{\Omega_d}\|^2 - \frac{1}{2\gamma_4} \|e_{\Omega_{dc}}\|^2 - \left(\frac{c_1 k_R}{\lambda_{\max}(J)} - \frac{c_1 k_\Omega}{2\lambda_{\min}(J)} - 2\alpha_1^2\right) \|e_{R_d}\|^2 \end{aligned} \quad (75)$$

From lemma (3) and using the properties of hyperbolic functions, we can state that for some $\|e_\alpha\| < \bar{e}_\alpha$, the function $\rho_1()$ is locally Lipschitz. Thus,

$$\|\hat{\Omega}_c\|^2 \leq L_1^2 \|e_\alpha\|^2 + \rho_{02}^2, \quad (76)$$

where L_1 , a function of \bar{e}_α is the Lipschitz constant and ρ_{02} is a positive constant. Substituting the (76) in (75) yields

$$\begin{aligned} \dot{V} \leq & -\underbrace{\left[mk_\alpha - \frac{m\alpha_x(3\alpha_x + 1)}{2} - \frac{m\alpha_f}{2} - \rho_{03}\right]}_{\lambda_1} \|e_\alpha\|^2 - \underbrace{\left[m\alpha_x - \frac{m\alpha_x^2}{2}\right]}_{\lambda_2} \|\tanh(e_x)\|^2 - \underbrace{\left[\frac{1}{2\gamma_3} - 2\alpha_1^2\right]}_{\lambda_4} \|e_{R_{dc}}\|^2 - \underbrace{\left[\frac{1}{2\gamma_4}\right]}_{\lambda_5} \|e_{\Omega_{dc}}\|^2 \\ & - \underbrace{\left[\frac{m\alpha_f}{2} - \frac{m\alpha_x}{2}\right]}_{\lambda_3} \|\tanh(e_f)\|^2 - \underbrace{\left[k_\Omega - \frac{c_1}{2} - \frac{c_1 k_\Omega}{2\lambda_{\min}(J)}\right]}_{\lambda_6} \|e_{\Omega_d}\|^2 - \underbrace{\left[\frac{c_1 k_R}{\lambda_{\max}(J)} - \frac{c_1 k_\Omega}{2\lambda_{\min}(J)} - 2\alpha_1^2\right]}_{\lambda_7} \|e_{R_d}\|^2 \\ & + \underbrace{\left[\left(\frac{\gamma_3}{2} + \frac{\gamma_4}{8\gamma_3^2}\right) \rho_{02}^2 + \frac{m}{2} \alpha_6^2\right]}_D, \end{aligned} \quad (77)$$

where $\rho_{03} = \frac{m}{2} + 1 + \frac{4\gamma_3^2 + \gamma_4}{8\gamma_3^2} L_1^2$. Equation (77) implies

$$\dot{V} \leq -\underbrace{\min(\lambda_1, \lambda_2, \lambda_3, \lambda_4, \lambda_5, \lambda_6, \lambda_7)}_{\lambda_v} \|e\|^2 + D \quad (78)$$

The relation (78) invokes uniformly ultimately bounded (UUB) stability since for $\|e(t)\|^2 > \frac{D}{\lambda_v}$, $\dot{V}(t)$ is negative-definite. However, note that (78) is derived based on (76), which demands $\|e_\alpha\| \leq \bar{e}_\alpha$. Hence, \bar{e}_α should be chosen such that $\bar{e}_\alpha \geq \sqrt{2 \frac{\max(V(0), \frac{D}{\lambda_v})}{m}}$, and accordingly the gain condition related to λ_1 has to be satisfied. This would ensure $\|e_\alpha(t)\| \leq \bar{e}_\alpha, \forall t \geq 0$, and hence, the UUB result would follow.

□

Remark 2. It's worth noting that D can be made arbitrarily small by choosing the filter gains $\gamma_1, \gamma_2, \gamma_{21}, \gamma_3, \gamma_4$ appropriately. This relaxes the unnecessary burden on the controller gains for such formulations. Moreover, if k_α is chosen such that the condition (41) is also satisfied then the desired attitude $R_c(t)$ always exists as $\|f_d(t)\| \geq \alpha_2 > 0$ is guaranteed.

5 | CONCLUSION

In this paper, we introduced a trajectory-tracking controller for multi-rotor unmanned aerial vehicles (UAVs) with limited knowledge of the desired trajectory, restricted to position and heading information. Using the auxiliary filter dynamics, the unavailability of the higher derivative of the desired trajectory is tackled to design both attitude and translational motion controllers hierarchically. It is theoretically shown that the designed thrust is saturated and always positive, avoiding singularities in the desired attitude construction. The designed controller has proven to be ultimately bounded in the extended error space considering attitude and position error dynamics through rigorous theoretical analysis.

Future work would focus on experimental validation and real-world implementations to further validate the controller's robustness and adaptability. Additionally, exploring potential enhancements to accommodate a desired trajectory with unbounded derivatives (i.e. relaxing Assumption 1) and external disturbances could further broaden the scope of applications for multi-rotor UAVs.

ACKNOWLEDGMENTS

This work is supported by TCS Research, India, under the TCS Research Scholar Program FP-140.

CONFLICT OF INTEREST

The authors declare no potential conflict of interests.

References

1. Idrissi M, Salami M, Annaz F. A review of quadrotor unmanned aerial vehicles: applications, architectural design and control algorithms. *Journal of Intelligent & Robotic Systems*. 2022;104(2):22.
2. Mahony R, Kumar V, Corke P. Multirotor Aerial Vehicles: Modeling, Estimation, and Control of Quadrotor. *IEEE Robotics & Automation Magazine*. 2012;19(3):20-32. doi: 10.1109/MRA.2012.2206474
3. Thomas J, Welde J, Loianno G, Daniilidis K, Kumar V. Autonomous flight for detection, localization, and tracking of moving targets with a small quadrotor. *IEEE Robotics and Automation Letters*. 2017;2(3):1762–1769.
4. Chen CW, Hung HA, Yang PH, Cheng TH. Visual Servoing of a Moving Target by an Unmanned Aerial Vehicle. *Sensors*. 2021;21(17). doi: 10.3390/s21175708
5. Tyagi P, Kumar Y, Sujit P. Nmpc-based uav 3d target tracking in the presence of obstacles and visibility constraints. In: IEEE. 2021:858–867.
6. Chen J, Liu T, Shen S. Tracking a moving target in cluttered environments using a quadrotor. In: IEEE. 2016:446–453.
7. Gomez-Balderas JE, Flores G, García Carrillo L, Lozano R. Tracking a ground moving target with a quadrotor using switching control: nonlinear modeling and control. *Journal of Intelligent & Robotic Systems*. 2013;70:65–78.
8. Li JM, Chen CW, Cheng TH. Motion Prediction and Robust Tracking of a Dynamic and Temporarily-Occluded Target by an Unmanned Aerial Vehicle. *IEEE Transactions on Control Systems Technology*. 2021;29(4):1623-1635. doi: 10.1109/TCST.2020.3012619
9. Serra P, Cunha R, Hamel T, Cabecinhas D, Silvestre C. Landing of a Quadrotor on a Moving Target Using Dynamic Image-Based Visual Servo Control. *IEEE Transactions on Robotics*. 2016;32:1524-1535. doi: 10.1109/TRO.2016.2604495
10. Jabbari Asl H. Robust vision-based tracking control of VTOL unmanned aerial vehicles. *Automatica*. 2019;107:425-432. doi: <https://doi.org/10.1016/j.automatica.2019.06.004>
11. Abdessameud A, Janabi-Sharifi F. Image-based tracking control of VTOL unmanned aerial vehicles. *Automatica*. 2015;53:111-119. doi: <https://doi.org/10.1016/j.automatica.2014.12.032>
12. Herissé B, Hamel T, Mahony R, Rusotto FX. Landing a VTOL unmanned aerial vehicle on a moving platform using optical flow. *IEEE Transactions on robotics*. 2011;28(1):77–89.

13. Sanchez-Lopez JL, Pestana J, Saripalli S, Campoy P. An approach toward visual autonomous ship board landing of a VTOL UAV. *Journal of Intelligent & Robotic Systems*. 2014;74:113–127.
14. Kumar Y, Roy S, Sujit P. Dynamic Image-Based Visual Servoing for Quadrotor to Track a Planar Target with Unknown Motion. In: IEEE. 2022:1398–1403.
15. Farrell JA, Polycarpou M, Sharma M, Dong W. Command Filtered Backstepping. *IEEE Transactions on Automatic Control*. 2009;54(6):1391–1395. doi: 10.1109/TAC.2009.2015562
16. Lin J, Wang Y, Miao Z, Wang H, Fierro R. Robust Image-Based Landing Control of a Quadrotor on an Unpredictable Moving Vehicle Using Circle Features. *IEEE Transactions on Automation Science and Engineering*. 2022.
17. Boss CJ, Srivastava V, Khalil HK. Robust tracking of an unknown trajectory with a multi-rotor UAV: A high-gain observer approach. In: IEEE. 2020:1429–1434.
18. Lee T, Leok M, McClamroch NH. Geometric tracking control of a quadrotor UAV on SE (3). In: IEEE. 2010:5420–5425.
19. Lee T. Exponential stability of an attitude tracking control system on SO(3) for large-angle rotational maneuvers. *Systems & Control Letters*. 2012;61(1):231–237. doi: <https://doi.org/10.1016/j.sysconle.2011.10.017>
20. Sharma M, Kar I. Nonlinear disturbance observer based geometric control of quadrotors. *Asian Journal of Control*. 2021;23(4):1936–1951. doi: <https://doi.org/10.1002/asjc.2318>
21. Emran BJ, Najjaran H. Global tracking control of quadrotor based on adaptive dynamic surface control. *International Journal of Dynamics and Control*. 2021;9:240–256.
22. Zhao S, Dong W, Farrell JA. Quaternion-based trajectory tracking control of VTOL-UAVs using command filtered backstepping. In: IEEE. 2013:1018–1023.
23. Dasgupta R, Roy SB, Patil OS, Bhasin S. A singularity-free hierarchical nonlinear quad-rotorcraft control using saturation and barrier lyapunov function. In: IEEE. 2019:3075–3080.
24. Zhang F, Dawson D, Queiroz dM, Dixon W. Global adaptive output feedback tracking control of robot manipulators. *IEEE Transactions on Automatic Control*. 2000;45(6):1203–1208. doi: 10.1109/9.863607
25. Khalil HK. Adaptive output feedback control of nonlinear systems represented by input-output models. *IEEE Transactions on Automatic Control*. 1996;41(2):177–188. doi: 10.1109/9.481517
26. Khalil HK. *Nonlinear systems; 3rd ed.* Upper Saddle River, NJ: Prentice-Hall, 2002.

How to cite this article: Kumar Y, Roy SB, and Sujit PB. Geometric Tracking Control of a Multi-rotor UAV for Partially Known Trajectories. *Int J Robust Nonlinear Control*. 2023;xx(xx):x–xx.

APPENDIX

A PRELIMINARIES ON ERROR FORMULATION ON SO(3)

To design the attitude tracking controller on a nonlinear space SO(3), we start with constructing a positive definite configuration error function Ψ . We then choose the configuration error vector and a velocity error vector in the tangent space $T_R\text{SO}(3)$ utilizing the derivatives of Ψ . Considering the carefully crafted error system, we design the controller following the Lyapunov direct method. Owing to the superior tracking performance for large initial attitude errors, we consider the following configuration error function¹⁹ $\Psi : \text{SO}(3) \times \text{SO}(3) \rightarrow \mathbb{R}$ for a given pair of desired attitude and angular velocity $R_1 \in \text{SO}(3)$, $\Omega_1 \in \mathbb{R}^3$, and the current attitude and angular velocity $R_2 \in \text{SO}(3)$, $\Omega_2 \in \mathbb{R}^3$

$$\Psi(R_2, R_1) = 2 - \sqrt{1 + \text{tr}[R_1^T R_2]}. \quad (\text{A1})$$

Based on the configuration error function, we define an attitude error vector $e_R(R_1, R_2) : \text{SO}(3) \times \text{SO}(3) \rightarrow \mathbb{R}^3$ and an angular velocity error vector $e_\Omega : \text{SO}(3) \times \mathbb{R}^3 \times \text{SO}(3) \times \mathbb{R}^3 \rightarrow \mathbb{R}^3$ as

$$e_R(R_2, R_1) = \frac{1}{2\sqrt{1 + \text{tr}[R_1^T R_2]}} (R_1^T R_2 - R_2^T R_1)^\vee, \quad (\text{A2})$$

$$e_\Omega(R_2, \Omega_2, R_1, \Omega_1) = \Omega_2 - R_2^T R_1 \Omega_1. \quad (\text{A3})$$

Throughout this article, we will use the following well-established properties¹⁹ of these error variables in a sub-level set $\mathcal{L}_2 = \{R_1, R_2 \in \text{SO}(3) | \Psi(R_2, R_1) < 2\}$ of Ψ

- Ψ is positive definite about $R_2 = R_1$ and has only one critical point $R_2 = R_1$.
- $\|e_R\|^2 \leq \Psi \leq 2\|e_R\|^2$.
- $\|e_R\| = \sin \frac{\|\theta\|}{2}$, where $\exp(\hat{\theta}) = R_1^T R_2$ i.e. $\|e_R\| < 1$.

The time derivative of the configuration function, attitude error and angular velocity $\Psi(R_2, R_1), e_R(R_2, R_1), e_\Omega(R_2, \Omega_2, R_1, \Omega_1)$ can be given as

$$\frac{d}{dt} \Psi(R_2, R_1) = e_R(R_2, R_1)^T e_\Omega(R_2, \Omega_2, R_1, \Omega_1), \quad (\text{A4})$$

$$\frac{d}{dt} e_R(R_2, R_1) = E(R_2, R_1) e_\Omega(R_2, \Omega_2, R_1, \Omega_1), \quad (\text{A5})$$

$$\frac{d}{dt} J e_\Omega(R_2, \Omega_2, R_1, \Omega_1) = J \dot{\Omega}_2 + J(\hat{\Omega}_2 R_2^T R_1 \Omega_1 - R_2^T R_1 \dot{\Omega}_1), \quad (\text{A6})$$

where $E(R_2, R_1) \in \mathbb{R}^{3 \times 3}$ is given as

$$E(R_2, R_1) = \frac{1}{2\sqrt{1 + \text{tr}[R_1^T R_2]}} (\text{tr}[R_2^T R_1] I - R_2^T R_1 + 2e_R e_R^T). \quad (\text{A7})$$

Using the fact that $\|E(R_2, R_1)\| = \frac{1}{2}$ from¹⁹, we can state that

$$\left\| \frac{d}{dt} e_R(R_2, R_1) \right\| \leq \frac{1}{2} \|e_\Omega(R_2, \Omega_2, R_1, \Omega_1)\|. \quad (\text{A8})$$

B PROOF OF LEMMAS

B.1 Lemma 1

Proof. From equation (17) we can write

$$\|f_d\| \leq mg + m\|g_1\| + 2m\|\tanh(e_x)\| + mk_\alpha \|\tanh(e_f)\|. \quad (\text{B9})$$

From the projection based differential estimate given in equation (23), we have $\|g_1\| \leq h_2$ and the fact that $\|\tanh(v)\| \leq 1 \forall v \in (-\infty, \infty)$, we can write

$$\|f_d\| \leq mg + mh_2 + 2\sqrt{3}m + m\sqrt{3}k_\alpha = \alpha_1. \quad (\text{B10})$$

Also, from the third row of equation (21) we get

$$f_{d_z} = mg - mg_{1_z} + 2m \tanh(e_{z_1}) - mk_\alpha \tanh(e_{f_z}) \quad (\text{B11})$$

Further calculating for the lower bound of the $f_{d_z}(t)$, we have

$$\|f_{d_z}\| \geq mg - mh_2 - 2m - mk_\alpha = \alpha_2. \quad (\text{B12})$$

α_2 is strictly positive for the given choice of k_α . □

B.2 Lemma 2

Proof. Substituting the expression of $f(t)$ in the expression of Δf , yields

$$\Delta f = \|f_d\| R_c e_3 - \|f_d\| \sqrt{\frac{1 + e_3^T R_c^T R_c e_3}{2}} R e_3, \quad (\text{B13})$$

The upper bound of the Δf can be calculated as

$$\|\Delta f\| \leq \left\| \|f_d\| R_c e_3 - \|f_d\| \sqrt{\frac{1 + e_3^T R_c^T R_c e_3}{2}} R e_3 \right\|. \quad (\text{B14})$$

Substituting the bounds of $\|f_d\|$ from lemma 1 to equation (B14)

$$\|\Delta f\| \leq \alpha_1 \left\| R_c e_3 - \sqrt{\frac{1 + e_3^T R_c^T R_c e_3}{2}} R e_3 \right\|. \quad (\text{B15})$$

The quantity $e_3^T R_c^T R_c e_3$ represents the cosine of the angle between vectors $R_c e_3$ and $R e_3$. Let the angle be θ' , then from equation (B15), we have

$$\|\Delta f\| \leq \alpha_1 \sqrt{1 - 2\cos\left(\frac{\theta'}{2}\right)\cos(\theta') + \cos^2\left(\frac{\theta'}{2}\right)}. \quad (\text{B16})$$

Using Rodrigues' formula, let's consider the following

$$R_c^T R = \exp(\hat{\theta}_1), \quad R_c^T R_d = \exp(\hat{\theta}_2) \quad R_d^T R = \exp(\hat{\theta}_3), \quad (\text{B17})$$

In the sublevel set \mathcal{L}_2 where $\theta' \leq \|\theta_1\|$ the following holds

$$\sqrt{1 - 2\cos\left(\frac{\theta'}{2}\right)\cos(\theta') + \cos^2\left(\frac{\theta'}{2}\right)} \leq 2\sin\left(\frac{\|\theta_1\|}{2}\right) = 2\|e_{R_c}\|. \quad (\text{B18})$$

Also, from (B17) we have

$$R_c^T R = (R_c^T R_d)(R_d^T R), \quad \exp(\hat{\theta}_1) = \exp(\hat{\theta}_2)\exp(\hat{\theta}_3), \quad \exp(\hat{\theta}_1) = \exp(\hat{\theta}_2 + \hat{\theta}_3). \quad (\text{B19})$$

From (B19), the following relation holds

$$\|\theta_1\| \leq \|\theta_2\| + \|\theta_3\|. \quad (\text{B20})$$

Since the attitude error is equal to $\sin\frac{\|\theta_i\|}{2}$ and in the sub-level set \mathcal{L}_2 i.e. $0 \leq \|\theta_i\| < \pi, \forall i = 1, 2, 3$, its monotonically increasing. Hence,

$$\|e_{R_c}\| \leq \|e_{R_{dc}}\| + \|e_{R_d}\|. \quad (\text{B21})$$

From equation (B21) and (B18), the bounds of $\|f_d\|$ can be given as

$$\|\Delta f\| \leq 2\alpha_1(\|e_{R_{dc}}\| + \|e_{R_d}\|), \quad (\text{B22})$$

□

B.3 Lemma 3

Proof. From (26) we have

$$\|\hat{\Omega}_c\| \leq \|\dot{R}_c\|. \quad (\text{B23})$$

The time derivative of R_c can be written as

$$\dot{R}_c = [\dot{x}_{B_c}, \dot{y}_{B_c}, \dot{z}_{B_c}], \quad (\text{B24})$$

where

$$\begin{aligned}\dot{z}_{B_c} &= \frac{\dot{f}_d}{\|f_d\|} - \frac{f_d(f_d^T \dot{f}_d)}{\|f_d\|^3}, \\ \dot{y}_{B_c} &= \frac{\dot{A}}{\|A\|} - \frac{(A^T \dot{A})}{\|A\|^3} A, \quad A = x_{B_d} \times z_{B_c} \\ \dot{x}_{B_c} &= \dot{y}_{B_c} \times z_{B_c} + y_{B_c} \times \dot{z}_{B_c}.\end{aligned}\tag{B25}$$

We individually calculate the upper bounds of column vectors of \dot{R}_c . The bounds on \dot{z}_{B_c} can be given as

$$\|\dot{z}_{B_c}\| \leq 2 \frac{\|\dot{f}_d\|}{\|f_d\|}\tag{B26}$$

Similarly, the bounds on \dot{y}_{B_c} can be given as

$$\|\dot{y}_{B_c}\| \leq 2 \frac{\|\dot{A}\|}{\|A\|}\tag{B27}$$

Since $x_{B_d} \nparallel z_{B_c}$, we have

$$\|\dot{y}_{B_c}\| \leq \frac{2}{\delta_A} (\|\dot{x}_{B_d}\| + \|\dot{z}_{B_c}\|),\tag{B28}$$

where $\delta_A \geq \|x_{B_d} \times z_{B_c}\|$. Using, equation (B25) and properties of SO(3) we can obtain the upper bound of \dot{x}_{B_c} as

$$\|\dot{x}_{B_c}\| \leq \|\dot{z}_{B_c}\| + \|\dot{y}_{B_c}\|\tag{B29}$$

Now, the upper bound of $\|\hat{\Omega}_c\|$ can be written as

$$\begin{aligned}\|\hat{\Omega}_c\| &\leq \|\dot{z}_{B_c}\| + \|\dot{y}_{B_c}\| + \|\dot{x}_{B_c}\| \\ &\leq 2\|\dot{z}_{B_c}\| + 2\|\dot{y}_{B_c}\| \\ &\leq (4 + \frac{4}{\delta_A}) \frac{\|\dot{f}_d\|}{\|f_d\|} + \frac{4}{\delta_A} h_5.\end{aligned}\tag{B30}$$

Let's evaluate the bound on the time derivatives of f_d . The time derivatives of f_d can be given as

$$\dot{f}_d = -m\dot{g}_1 + 2m\text{Sech}^2(e_x)\dot{e}_x - mk_\alpha\text{Sech}^2(e_f)\dot{e}_f.\tag{B31}$$

Substituting the expressions from (15), (23) and (31) in the (B31) will yield

$$\dot{f}_d = -m\phi + m\Phi_{g_1} + 2m\text{Sech}^2(e_x)(e_\alpha - \alpha_x \tanh(e_x) - \tanh(e_f)) + mk_\alpha^2 e_\alpha - mk_\alpha \tanh(e_x) + mk_\alpha \alpha_f \tanh(e_f).\tag{B32}$$

The quantity Φ_{g_1} can be bounded as

$$\begin{aligned}\|\Phi_{g_1}\| &\leq \frac{\|\nabla f(g_1)\|^2}{\|\nabla f(g_1)\|^2} \|\phi\| \|f(g_1)\|, \\ &\leq \|\phi\| \|f(g_1)\|,\end{aligned}\tag{B33}$$

and Φ_{g_1} appears when $f(g_1) > 0$ (i.e. $h_2 < \|g_1\| < h_2 + \epsilon_0$), then

$$\|\Phi_{g_1}\| \leq \|\phi\| \frac{\epsilon_0 + 2h_2}{h_2^2},\tag{B34}$$

where ϕ can be written in the form of filter errors as

$$\phi = \frac{1}{\gamma_{21}} (e_{g_1} - e_{g_v} - e_{\dot{x}_d}).\tag{B35}$$

Then from equation (36) and (B32), we can write

$$\begin{aligned} \|\dot{f}_d\| \leq & \frac{m}{\gamma_{21}} \left(1 + \frac{\epsilon_0 + 2h_2}{h_2^2} \right) (\|e_{g_1}\| + \|e_{g_v}\| + \|e_{\ddot{x}_d}\|) + 2m (\|e_\alpha\| + \alpha_x \|\tanh(e_x)\| + \|\tanh(e_f)\|) \\ & + mk_\alpha^2 \|e_\alpha\| + mk_\alpha \|\tanh(e_x)\| + mk_\alpha \alpha_f \|\tanh(e_f)\|. \end{aligned} \quad (\text{B36})$$

Using lemma 1, 4 and relation (B36), the equation (B30) can be written as

$$\|\hat{\Omega}_c\| \leq \rho_1(\|e_\alpha\|, \|\tanh(e_x)\|, \|\tanh(e_f)\|) + \rho_{01}, \quad (\text{B37})$$

where $\rho_1()$ is class κ -function and ρ_{01} is a positive constant. \square

B.4 Lemma 4

Proof. For the error e_{g_x} , lets consider the following Lyapunov candidate

$$V_{g_x} = \frac{1}{2} e_{g_x}^T e_{g_x}. \quad (\text{B38})$$

Taking the time derivative of $V_{g_x}(t)$ and using (37) will yield

$$\dot{V}_{g_x} = -\frac{1}{\gamma_1} e_{g_x}^T e_{g_x} + e_{g_x}^T \ddot{x}_d. \quad (\text{B39})$$

This implies that

$$\|e_{g_x}\| = \sqrt{2V_{g_x}(t)} \leq \sqrt{\|e_{g_x}(0)\|^2 \exp\left(-\frac{1}{\gamma_1} t\right) + \gamma_1^2 h_2^2}. \quad (\text{B40})$$

Similarly, for error $e_{\ddot{x}_d}(t)$, consider the following Lyapunov candidate

$$V_{\ddot{x}_d} = \frac{1}{2} e_{\ddot{x}_d}^T e_{\ddot{x}_d}. \quad (\text{B41})$$

Taking the time derivative of $V_{\ddot{x}_d}(t)$ and using (37) will yield

$$\dot{V}_{\ddot{x}_d} = -\frac{1}{\gamma_1} e_{\ddot{x}_d}^T e_{\ddot{x}_d} + e_{\ddot{x}_d}^T \ddot{x}_d. \quad (\text{B42})$$

This implies that

$$\|e_{\ddot{x}_d}\| = \sqrt{2V_{\ddot{x}_d}(t)} \leq \sqrt{\|e_{\ddot{x}_d}(0)\|^2 \exp\left(-\frac{1}{\gamma_1} t\right) + \gamma_1^2 h_3^2}. \quad (\text{B43})$$

For error e_{g_v} , consider the following Lyapunov candidate

$$V_{g_v} = \frac{1}{2} e_{g_v}^T e_{g_v}. \quad (\text{B44})$$

Taking the time derivative of $V_{g_v}(t)$ and using (37) will yield

$$\dot{V}_{g_v} = -\frac{1}{\gamma_2} e_{g_v}^T e_{g_v} + \frac{1}{\gamma_1} e_{g_v}^T e_{\ddot{x}_d}. \quad (\text{B45})$$

This implies that

$$\|e_{g_v}\| = \sqrt{2V_{g_v}(t)} \leq \sqrt{\|e_{g_v}(0)\|^2 \exp\left(-\frac{1}{\gamma_2} t\right) + \frac{\gamma_2^2}{\gamma_1^2} \|e_{\ddot{x}_d}\|^2}. \quad (\text{B46})$$

Finally, we will analyze the dynamical behavior of the error $e_{g_1}(t)$ by choosing the following Lyapunov candidate

$$V_{g_1} = \frac{1}{2} e_{g_1}^T e_{g_1}. \quad (\text{B47})$$

Taking the time derivative of $V_{g_1}(t)$ and using (37) will yield

$$\dot{V}_{g_1} = -\frac{1}{\gamma_{21}} e_{g_1}^T e_{g_1} + \frac{1}{\gamma_{21}} e_{g_1}^T e_{g_v} + \frac{1}{\gamma_{21}} e_{g_1}^T e_{\dot{x}_d} + e_{g_1}^T \Phi_{g_1} + e_{g_1}^T \ddot{x}_d. \quad (\text{B48})$$

Using the fact that $e_{g_1}^T \Phi_{g_1} \leq 0$, the bounds on $\dot{V}_{g_1}(t)$ can be given as

$$\dot{V}_{g_1} \leq -\frac{1}{2\gamma_{21}} \|e_{g_1}\|^2 + \frac{2}{\gamma_{21}} \|e_{g_v}\|^2 + \frac{2}{\gamma_{21}} \|e_{\dot{x}_d}\|^2 + \gamma_{21} h_3^2. \quad (\text{B49})$$

Solving (B49) for $V_{g_1}(t)$ using equations (45), (46)

$$V_{g_1}(t) \leq V_{g_1}(0) \exp\left(-\frac{1}{\gamma_{21}} t\right) + 4\alpha_4^2 + 4\alpha_5^2 + \gamma_{21}^2 h_3^2. \quad (\text{B50})$$

This implies that

$$\|e_{g_1}(t)\| = \sqrt{2V_{g_1}(t)} \leq \sqrt{\|e_{g_1}(0)\|^2 \exp\left(-\frac{1}{\gamma_{21}} t\right) + \alpha_7}, \quad (\text{B51})$$

where $\alpha_7 = 8(\alpha_4^2 + \alpha_5^2) + 2\gamma_{21}^2 h_3^2$. □